

TWO-DIMENSIONAL RMSD PROJECTIONS FOR REACTION PATH VISUALIZATION AND VALIDATION

A PREPRINT

 **Rohit Goswami***

Institute IMX and Lab-COSMO
École polytechnique fédérale de Lausanne (EPFL)
Station 12, CH-1015 Lausanne, Switzerland
and
TurtleTech ehf., 107 Reykjavík, Iceland
rgoswami@ieee.org

December 9, 2025

ABSTRACT

Transition state or minimum energy path finding methods constitute a routine component of the computational chemistry toolkit. Standard analysis involves trajectories conventionally plotted in terms of the relative energy to the initial state against a cumulative displacement variable, or the image number. These dimensional reductions obscure structural rearrangements in high dimensions and may often be trajectory dependent. This precludes the ability to compare optimization trajectories of different methods beyond the number of calculations, time taken, and final saddle geometry. We present a method mapping trajectories onto a two-dimension surface defined by a permutation corrected root mean square deviation from the reactant and product configurations. Energy is represented as an interpolated color-mapped surface constructed from all optimization steps using radial basis functions. This representation highlights optimization trajectories, identifies endpoint basins, and diagnoses convergence concerns invisible in one-dimensional profiles. We validate the framework on a cycloaddition reaction, showing that a machine-learned potential saddle and density functional theory reference lie on comparable energy contours despite geometric displacements.

Keywords Nudged Elastic Band, Saddle Search Methods, Visualization, Transition States

A core component of any chemical study involves the determination of reactive pathways. Within the harmonic transition state theory approximation, this simplifies to the determination of the saddle point geometry between two known minima. The nudged elastic band method [6] coupled with the climbing image [5] and spring variations [1] with local accelerations [3, 7] and the string family of methods [9, 11, 12] form the current Pareto optimal forms.

The interpretation of the resulting trajectories often ends up oversimplified. One dimensional “profile” plots commonly show only the final optimized path, either against the image number², which obscures any distance measure between the images. An improvement to this involves the cubic Hermite interpolation [5] involving the forces relative to the “reaction coordinate,” defined by the piece-wise sum of the Euclidean distances between intermediate images. The reaction coordinate $s_i = \sum_{j=1}^i \|\mathbf{R}_j - \mathbf{R}_{j-1}\|_2$ depends entirely on the specific path geometry and optimization history. This scalar measure lacks a unique definition and collapses global geometric information onto a single, arbitrary axis. This dimensional reduction precludes rigorous comparison between trajectories generated by differing algorithms—such as NEB versus Frozen String methods—or even identical algorithms with varying parameters. Furthermore, the one-dimensional projection frequently masks the distinction between numerical instability and physical relaxation into alternative basins, creating ambiguity in the validation of stationary points which costs researchers often days of calculations to clarify.

*Corresponding Author

²e.g. as found in ASE [8]

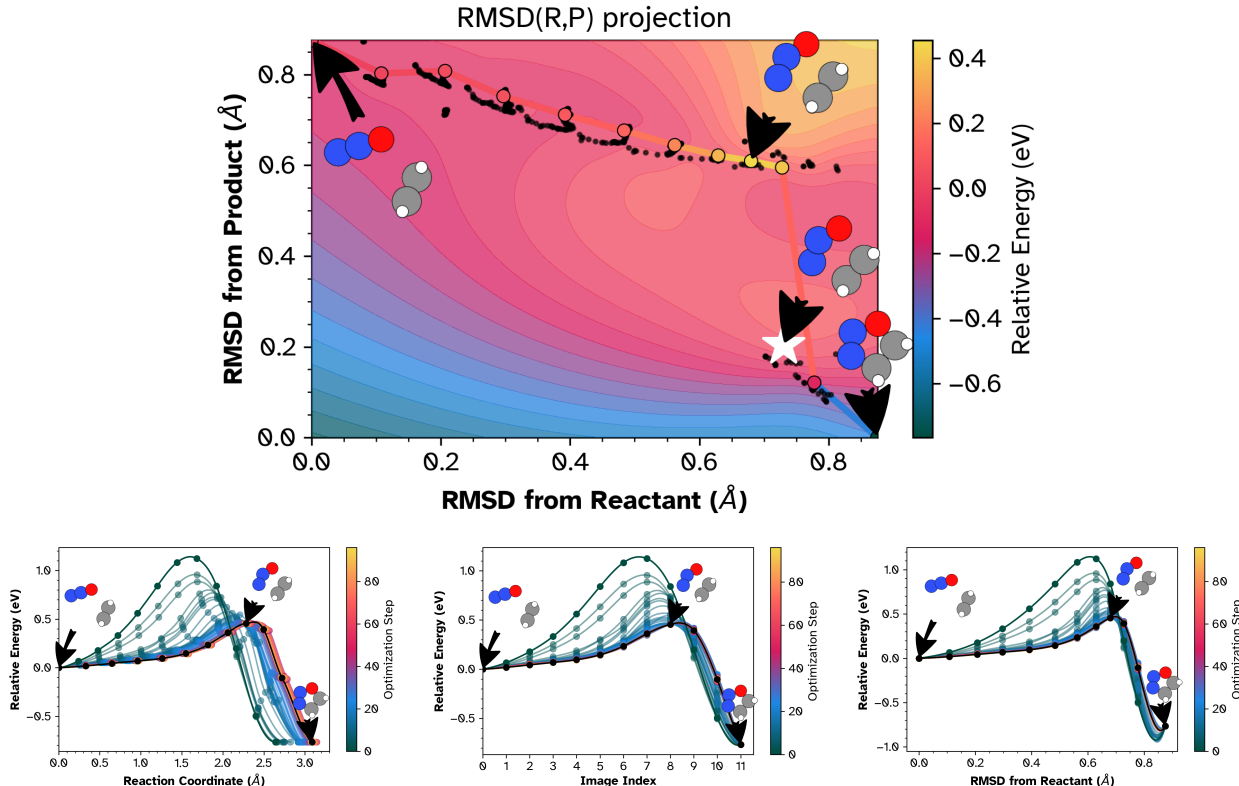


Figure 1: NEB optimization of ethylene + N_2O cycloaddition using PET-MAD v1.1 potential. **Top:** 2D RMSD projection showing interpolated energy landscape (color), sampled structures (black dots), and converged path (open circles). White star indicates ORCA B3LYP-D3 saddle. **Bottom left:** Energy vs. reaction coordinate. **Bottom center:** Energy vs. image index. **Bottom right:** Energy vs. RMSD from reactant. In all panels, colored curves show optimization progression (dark \rightarrow light = early \rightarrow late); final path in black. The 2D projection reveals landscape topology and enables reference structure assessment impossible in 1D profiles.

To establish a method-agnostic framework for analysis, we map the optimization trajectory onto a two-dimensional surface defined by the intrinsic geometric distance from the limiting stationary points: the reactant (**R**) and product (**P**). We define coordinates as $(d_{\text{RMSD}}(\mathbf{X}, \mathbf{R}), d_{\text{RMSD}}(\mathbf{X}, \mathbf{P}))$ where

$$d_{\text{RMSD}}(\mathbf{A}, \mathbf{B}) = \min_{\mathbf{R}, \mathbf{P}} \sqrt{\frac{1}{N} \sum_{j=1}^N \|\mathbf{R}\mathbf{a}_{\mathbf{P}(j)} - \mathbf{b}_j\|^2} \quad (1)$$

with optimal permutation **P** and rotation **R** determined via the Iterative Rotations and Assignments (IRA) algorithms [4] algorithm. This procedure guarantees unique, invariant coordinates regardless of the initial atom indexing or frame orientation. The discrete optimization steps provide a sparse sampling of this geometric subspace.

To visualize the underlying potential energy landscape, we construct a continuous perceptually uniform color-mapped surface using radial basis function (RBF) interpolation of the energies sampled throughout the optimization history. The discrete optimization samples we interpolate using thin-plate spline functions with smoothing parameter $\lambda = L/100$, where $L = \max(\text{RMSD}_R^{\max}, \text{RMSD}_P^{\max})$ forms the domain extent. This choice provides a smoothing length scale of approximately 1% of the coordinate range, suppressing noise from sparse sampling while preserving essential landscape topology. This visualization displays the convergence dynamics and the contours of the explored energy surface, while highlighting the final path with insets for saddle points and additional reference structures.

We validate the framework on the 1,3-dipolar cycloaddition of ethylene and N_2O forming 4,5-dihydro-1,2,3-oxadiazole, a well-studied benchmark reaction for NEB method development [1, 2, 7]. Figure~1 compares conventional one-dimensional representations with the two-dimensional RMSD projection for energy-weighted NEB optimization in

EON³ using the PET-MAD machine-learned potential [10] using Metatomic [2]. PET-MAD has been trained on PBESol reference data. We contrast this with a saddle optimized from a different NEB calculation using the B3LYP functional in ORCA [1] projected onto the interpolated landscape (white star).

The conventional profiles (Fig.1, bottom) show optimization from an initial barrier of approximately 1.1~eV to a final value near 0.4eV over 120 steps, with the product lying approximately 0.8~eV below the reactant. The final path (black) appears smooth and well-converged. These representations provide no information about sampling quality or the broader landscape topology.

The two-dimensional RMSD projection (Fig.1, top) provides some more insight. First, sampled structures (black dots) cluster tightly along the converged path, confirming robust single-pathway convergence without geometric wandering. Second, the interpolated energy surface displays clear landscape topology: a barrier region (yellow/orange, approximately 0.4eV) separating the reactant basin (upper-left) from the deeper product basin (blue, lower-right). Third, the path’s trajectory deviates from the diagonal, with RMSD_P decreasing more rapidly than RMSD_R increases near the product. This asymmetry captures the specific geometric character of the cycloaddition, where ring formation proceeds concurrently with N–O bond rearrangement, yet the system geometrically resembles the product before fully departing the reactant configuration.

Furthermore, this framework provides a unified coordinate system for validating potential energy surfaces against higher-level theory. We projected a DFT reference saddle onto the interpolated MLIP landscape (Fig. 1 top, white star). The PET-MAD climbing image locates the saddle at approximately (0.5, 0.65) Å in RMSD coordinates, while the DFT reference lies at (0.65, 0.22) Å. We note that the PET-MAD potential relies on PBESol training data, whereas the reference saddle derives from B3LYP-D3 calculations. Consequently, the observed geometric displacement of ≈ 0.4 Å reflects the genuine physical difference between the PET-MAD and B3LYP-D3 potential energy surfaces rather than an optimization failure. Despite this shift, the projection reveals that the ORCA saddle configuration falls within comparable energy contours (pink region, ≈ -0.2 to 0.0 eV) as the adjacent PET-MAD path. The reference avoids both the deep product basin and the highest barrier region, landing instead in the transition zone. This placement visually confirms that PET-MAD captures the qualitative barrier topology even if the precise saddle geometry differs due to functional sensitivity. This assessment would be impossible with conventional one-dimensional profiles.

Conclusion

We presented a coordinate-free visualization method for analyzing reaction path optimization trajectories. By projecting high-dimensional pathways onto a surface defined by permutation-invariant RMSD coordinates, the method reveals geometric and energetic features obscured by standard one-dimensional profiles. The cycloaddition benchmark demonstrates the capacity of this representation to distinguish numerical artifacts from physical topology and to study differences in potential energy surfaces, with an eye towards validating machine learning potentials. This visualization enables validation of saddle point searches beyond point comparisons of geometry and the comparison of diverse saddle finding algorithms on a unified geometric basis. Finally, while we focus on double-ended methods here, the (RMSD_R , RMSD_P) projection operates independently of the path generation algorithm. One can project trajectories from single-ended saddle search methods, molecular dynamics, or meta-dynamics onto these intrinsic axes post-hoc to diagnose path quality and hysteresis with a destination basin.

Conflict of Interest

We declare no conflicts of interest.

References

- [1] ÁSGEIRSSON, V., BIRGISSON, B. O., BJORNSSON, R., BECKER, U., NEESE, F., RIPLINGER, C., AND JÓNSSON, H. Nudged Elastic Band Method for Molecular Reactions Using Energy-Weighted Springs Combined with Eigenvector Following. *Journal of Chemical Theory and Computation* 17, 8 (Aug. 2021), 4929–4945.
- [2] BIGI, F., ABBOTT, J. W., LOCHE, P., MAZITOV, A., TISI, D., LANGER, M. F., GOSCINSKI, A., PEGOLO, P., CHONG, S., GOSWAMI, R., CHORNA, S., KELLNER, M., CERIOTTI, M., AND FRAUX, G. Metatensor and metatomic: Foundational libraries for interoperable atomistic machine learning, Aug. 2025.

³from <https://eondocs.org>

- [3] GOSWAMI, R., MASTEROV, M., KAMATH, S., PENA-TORRES, A., AND JÓNSSON, H. Efficient Implementation of Gaussian Process Regression Accelerated Saddle Point Searches with Application to Molecular Reactions. *Journal of Chemical Theory and Computation* (July 2025).
- [4] GUNDE, M., SALLES, N., HÉMERYCK, A., AND MARTIN-SAMOS, L. IRA: A shape matching approach for recognition and comparison of generic atomic patterns. *Journal of Chemical Information and Modeling* 61, 11 (Nov. 2021), 5446–5457.
- [5] HENKELMAN, G., UBERUAGA, B. P., AND JÓNSSON, H. A climbing image nudged elastic band method for finding saddle points and minimum energy paths. *The Journal of Chemical Physics* 113, 22 (Nov. 2000), 9901–9904.
- [6] JONSSON, H., MILLS, G., AND JACOBSEN, K. W. Nudged elastic band method for finding minimum energy paths of transitions. In *Classical and Quantum Dynamics in Condensed Phase Simulations*. World Scientific, June 1998, pp. 385–404.
- [7] KOISTINEN, O.-P., ÁSGEIRSSON, V., VEHTARI, A., AND JÓNSSON, H. Nudged Elastic Band Calculations Accelerated with Gaussian Process Regression Based on Inverse Interatomic Distances. *Journal of Chemical Theory and Computation* 15, 12 (Dec. 2019), 6738–6751.
- [8] LARSEN, A. H., MORTENSEN, J. J., BLOMQVIST, J., CASTELLI, I. E., CHRISTENSEN, R., DULAK, M., FRIIS, J., GROVES, M. N., HAMMER, B., HARGUS, C., HERMES, E. D., JENNINGS, P. C., JENSEN, P. B., KERMODE, J., KITCHIN, J. R., KOLSBJERG, E. L., KUBAL, J., KAASBJERG, K., LYSGAARD, S., MARONSSON, J. B., MAXSON, T., OLSEN, T., PASTEWKA, L., PETERSON, A., ROSTGAARD, C., SCHIØTZ, J., SCHÜTT, O., STRANGE, M., THYGESEN, K. S., VEGGE, T., VILHELMSSEN, L., WALTER, M., ZENG, Z., AND JACOBSEN, K. W. The atomic simulation environment—a Python library for working with atoms. *Journal of Physics: Condensed Matter* 29, 27 (June 2017), 273002.
- [9] MARKS, J., AND GOMES, J. Incorporation of Internal Coordinates Interpolation into the Freezing String Method. *Journal of Chemical Theory and Computation* (Nov. 2025).
- [10] MAZITOV, A., BIGI, F., KELLNER, M., PEGOLO, P., TISI, D., FRAUX, G., POZDNYAKOV, S., LOCHE, P., AND CERIOTTI, M. PET-MAD, a universal interatomic potential for advanced materials modeling, Mar. 2025.
- [11] PETERS, B., HEYDEN, A., BELL, A. T., AND CHAKRABORTY, A. A growing string method for determining transition states: Comparison to the nudged elastic band and string methods. *The Journal of Chemical Physics* 120, 17 (May 2004), 7877–7886.
- [12] ZIMMERMAN, P. M. Growing string method with interpolation and optimization in internal coordinates: Method and examples. *The Journal of Chemical Physics* 138, 18 (May 2013), 184102.